

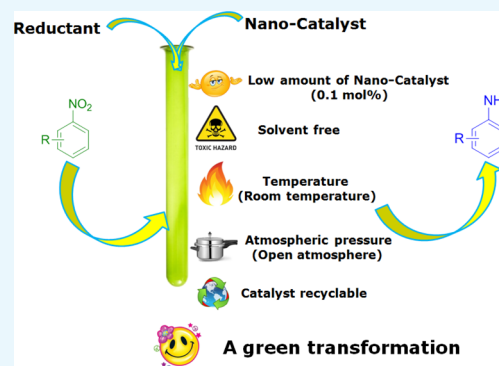
Bimetallic Pd–Au/TiO₂ Nanoparticles: An Efficient and Sustainable Heterogeneous Catalyst for Rapid Catalytic Hydrogen Transfer Reduction of Nitroarenes

Bhairi Lakshminarayana, Gedu Satyanarayana,*^{ORCID} and Challapalli Subrahmanyam*^{ORCID}

Department of Chemistry, Indian Institute of Technology Hyderabad, Kandi, Sangareddy, 502285 Telangana, India

S Supporting Information

ABSTRACT: Anilines are one of the important chemical feedstocks and are utilized for the preparation of a variety of pharmaceuticals, agrochemicals, pigments, and dyes. In this context, the catalytic reduction of nitro functionality is an industrially vital process for the synthesis of aniline derivatives. Herein, we report an efficient nanosized bimetallic Pd–Au/TiO₂ nanomaterial which is proved to be quite efficient for rapid catalytic hydrogen transfer reduction of nitroarenes into corresponding amines. Significantly, the reduction process is successful under solvent-free and mild green atmospheric conditions. Bimetallic Pd–Au nanoparticles served as the active center, and TiO₂ played as a support in hydrogen transfer from the source hydrazine monohydrate. Typical results highlighted that the reactions were very rapid and the products were obtained in good to excellent yields. Significantly, the process was successful in the presence of a very low amount catalyst (0.1 mol %). Furthermore, the reaction showed good chemoselectivity and compatibility with double or triple bond, aldehyde, ketone, and ester functionalities on the aromatic ring. Typical results indicated the true heterogeneous nature of the Pd–Au/TiO₂ nanocatalyst, where the catalyst retained the activity, without loss of its activity.



INTRODUCTION

Development of a green protocol for organic transformations is a great challenge to the synthetic community. A catalyst is a necessary element of any sustainable development.¹ In this context, development of stable, highly active, recyclable, and environmentally benign catalysts is highly desirable. Nanomaterial-based catalysts act as viaducts between homogeneous and heterogeneous catalysts and promote the advantages, namely, selectivity and recyclability.^{2,3} Therefore, nanocatalysts play an important role in the development of sustainable processes.^{4,5} Noble metal-containing nanomaterials have attracted a significant consideration because of their unique physicochemical properties, which exhibit versatile applications in organic transformations.^{6–8} It is desirable to have high dispersion of noble metals such as Pd, Au, Pt, and so forth, which is an important issue in the field of heterogeneous catalysis.⁹ Bimetallic nanomaterials have recently attracted an extensive consideration because of their enhanced catalytic properties when compared to monometallic nanoparticles for several catalytic reactions.^{10–21}

Reduction of nitroarenes to the corresponding aniline derivatives is essential for various industrial applications such as the preparation of pharmaceuticals, pigments, agrochemicals, dyestuffs, and polymers.^{22–24} The environmentally benign and selective reduction of the nitro group with other easily reducible groups (double or triple bonds and carbonyl groups) of aromatic derivatives is a challenge. Heterogeneous

catalytic reduction of nitroarenes is rather preferred with regard to high yields and selectivity over traditional metal-mediated reductions (iron, zinc, and tin).²⁵ In addition, heterogeneous catalytic reduction of nitroarenes, particularly, working under ligand and solvent-free and at milder reaction conditions is advantageous than those that make use of high pressure reactors of hydrogen gas,^{26,27} toxic organic solvents, ligands, and high temperatures.^{24,28} The catalytic reduction of nitroarenes mediated by homogeneous transition-metal catalysts has also been well-established (i.e. Pd,^{29,30} Ru,³¹ Rh,³² Ir,³³ and Ni³⁴). However, the main limitation of homogeneous catalysts is recyclability and reusability, whereas the commercially available heterogeneous catalysts (Pd/C) are less efficient because a high amount of noble metals is required.³⁵ However, the separation of nanocatalysts is difficult because of its small size.^{36,37} To overcome this problem, nanoparticles supported on high surface area materials is often practiced. To the best of our knowledge, a few reports are accessible for the combination of bimetallic metals and metal oxide supports for nitroarenes reduction reactions.^{16,17}

Herein, we report a highly active bimetallic Pd–Au supported by a TiO₂ heterogeneous catalyst, which exhibits higher activity on the reduction of nitroarenes into anilines.

Received: August 16, 2018

Accepted: September 27, 2018

Published: October 11, 2018

The catalytic activity of bimetallic Pd–Au/TiO₂ has been studied on hydrogenation of nitroarenes under mild and solvent-free green atmospheric conditions. The efficacy of the developed Pd–Au/TiO₂ catalyst has been confirmed by comparing with monometallic Pd/TiO₂ and Au/TiO₂ catalysts. In addition, chemoselectivity and recyclability of the Pd–Au/TiO₂ catalyst has also been examined.

RESULTS AND DISCUSSION

Synthesis of TiO₂-Supported Pd Nanoparticles. A mixture of PdCl₂ (0.56 mmol, 100 mg) and NaCl (1.5 mmol, 88 mg) was taken in 10 mL of methanol and stirred continuously for 24 h at room temperature. It was then diluted with 40 mL of methanol and stirred for 5 min at room temperature, and TiO₂ nanoparticles (6.26 mmol, 500 mg) were added into this solution. Further, the resultant mixture was stirred continuously for 1 h at 60 °C. Finally, the reaction mixture was cooled to room temperature, and sodium acetate (9.26 mmol, 0.76 g) and 0.5 mL of hydrazine monohydrate were added to into the mixture and stirred for 1 h. At the end, the mixture was centrifuged with methanol, water, and acetone. It was kept in the oven for drying, followed by grinding to obtain a fine powder.

Synthesis of TiO₂-Supported Pd–Au Nanoparticles. A mixture of PdCl₂ (0.56 mmol, 100 mg), HAuCl₄ (0.56 mmol, 190 mg), and NaCl (1.5 mmol, 88 mg) was taken in 10 mL of methanol and stirred continuously for 24 h at room temperature. It was then diluted with 40 mL of methanol and stirred for 5 min at room temperature, and TiO₂ nanoparticles (6.26 mmol, 500 mg) were added into this solution. Further, the resultant mixture was stirred continuously for 1 h at 60 °C. Finally, the reaction mixture was cooled to room temperature, and sodium acetate (9.26 mmol, 0.76 g) and 0.5 mL of hydrazine monohydrate were added to into the mixture and stirred for 1 h. At the end, the mixture was centrifuged with methanol, water, and acetone and kept in the oven for drying.

Characterization of As-Prepared Catalysts. *X-ray Diffraction (XRD).* The powder XRD patterns of pure TiO₂, Pd/TiO₂, and Pd–Au/TiO₂ are shown in Figure 1, which confirmed the formation of the catalysts. By using the JCPDS no.: 89–4921 (TiO₂), 89–4897 (Pd), and 89–3697 (Au), the presence of the active components is identified. The diffraction peaks of pure TiO₂ showed *d*-spacing values of 3.509, 2.426, 2.375, 2.328, 1.888, 1.697, 1.662, 1.490, and 1.478 Å representing (101), (103), (004), (112), (200), (105),

(211), (204), and (116) crystalline planes, respectively.^{38–40} In a similar manner, the peaks of Pd showed *d*-spacing values of 2.245, 1.948, 1.375, and 1.663 Å corresponding to (111), (200), (220), and (311) crystalline planes, respectively, and the peaks of Au showed *d*-spacing values of 2.339, 1.939, 1.439, 1.229, and 1.164 Å representing (111), (200), (220), (311), and (222) crystalline planes, respectively.^{41–43}

Raman Analysis. The Raman spectra of TiO₂, Pd/TiO₂, and Pd–Au/TiO₂ indicated E_g, B_{1g}, and A_{1g} peaks. The E_g peak is due to the symmetrical stretching vibrations of O–Ti–O, whereas the B_{1g} peak is due to the symmetrical bending vibrations of O–Ti–O and the A_{1g} peak is due to asymmetric bending vibrations of O–Ti–O in the TiO₂ nanoparticles. In Figure 2, fresh TiO₂ has five Raman active modes in the vibrational spectrum centered at 143, 196, 395, 514, and 636 cm^{−1}, which are assigned to the E_g, E_g, B_{1g}, A_{1g}, and E_g symmetries of the anatase phase of TiO₂.^{44,45} Pd impregnated on TiO₂ showed Raman vibrational modes centered at 152, 205, 237, 268, 330, 401, 562, 617, and 692 cm^{−1} because of A_{1g}, B_{1g}, A_{1g}, B_{3g}, B_{1g}, A_{1g}, B_{3g}, A_{1g}, and A_g symmetries of the

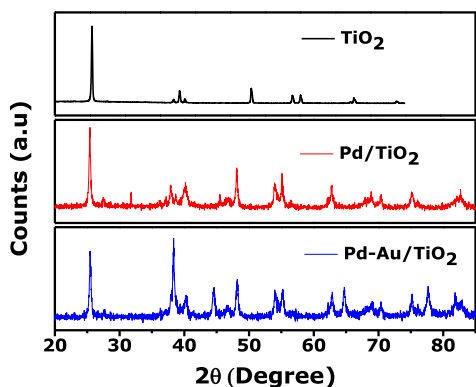


Figure 1. XRD pattern of TiO₂, Pd/TiO₂ and Pd–Au/TiO₂.

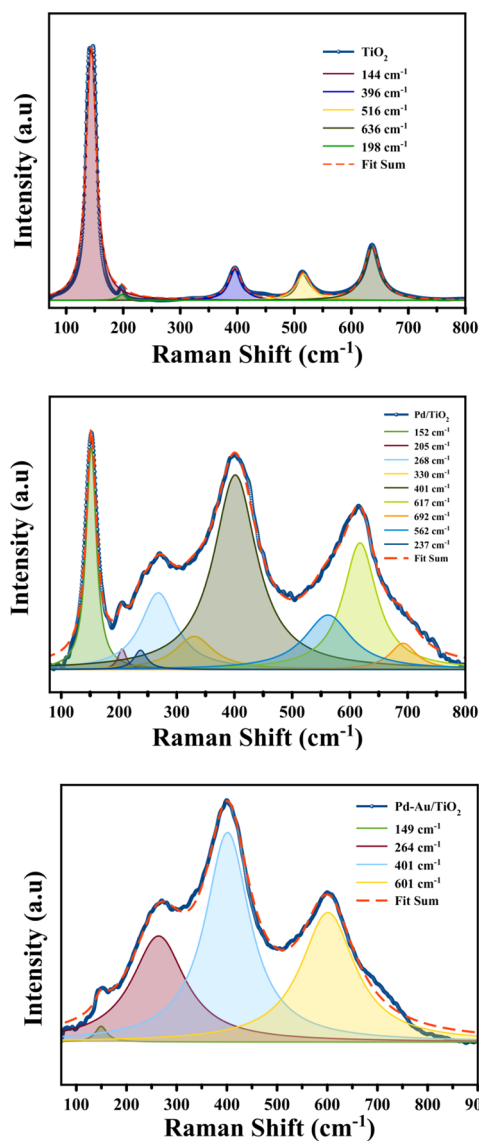


Figure 2. Raman spectra of TiO₂, Pd/TiO₂, and Pd–Au/TiO₂ nanomaterials.

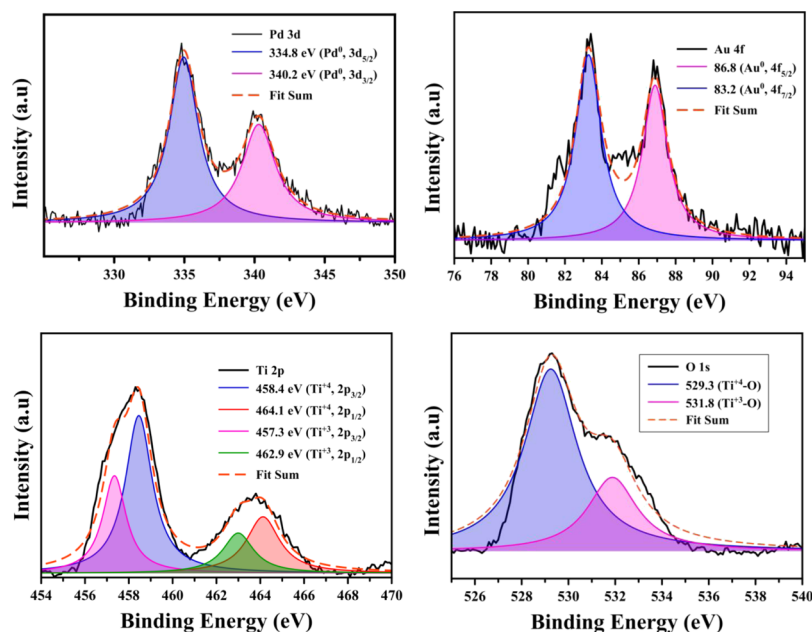


Figure 3. XPS pattern of as-prepared Pd–Au/TiO₂ nanomaterials.

Brookite phase of Pd/TiO₂, respectively,^{46–55} whereas Pd–Au-impregnated TiO₂ showed the Raman vibrational modes at 149, 264, 401, and 601 cm^{−1} corresponding to the B_{1g} and two phonon scattering E_g and A_{1g} modes of the rutile phase of Pd–Au/TiO₂, respectively.^{56,57} The phase transformation of TiO₂ in Pd/TiO₂ and Pd–Au/TiO₂ is due to the presence of NaCl and NaOAc in the synthesis, which favors the anatase–brookite and anatase–rutile phases of TiO₂. With the introduction of NaCl and NaOAc, the Na⁺ ions locally stops the direct closure of titanate layers at their adjacent positions, which induces the brookite- and rutile-like structures.^{58,59}

XPS Analysis. The valence states of the Pd–Au/TiO₂ nanocatalyst were analyzed by X-ray photoelectron spectroscopy (XPS). The XPS spectra shown in Figure 3 show the characteristic Pd 3d_{5/2} and Pd 3d_{3/2} peaks at 339.6 and 335.7 eV, respectively, corresponding to Pd(0).⁶⁰ The XPS core level spectra of the Au 4f are shown in Figure 3. The binding energies (BEs) of Au 4f_{7/2} and Au 4f_{5/2} electrons are 83.2 and 86.8 eV, respectively. It is reliable with the reports on gold metal, which indicate that in Pd–Au/TiO₂, Au exists in the metallic state (Au(0)).⁶¹ The valence state of nonstoichiometric TiO₂ in Pd–Au/TiO₂ was confirmed by XPS analysis of Ti 2p and O 1s peaks coupled with Lorentzian fits shown in Figure 3.⁶² The peaks centered at 457.3 and 458.4 eV are due to Ti₂O₃ and TiO₂ species, respectively.^{61,63} This is also supported by the deconvoluted O 1s spectrum, which revealed the BE of the individual Ti(III) at 531.8 eV (Ti³⁺–O) and Ti(IV) at 529.3 eV (Ti⁴⁺–O).⁶⁴

Transmission Electron Microscopy (TEM) Analysis. Figure 4 shows the morphological characteristics of Pd–Au nanoparticles on TiO₂ nanoparticles. The average particle size of Pd–Au nanoparticles is 5 nm, and TiO₂ nanoparticles exhibited a wide range of sizes. We observed from the images that the particles mostly have spherical shape.

Catalytic Activity. In an oven-dried 10 mL test tube, nitroarenes **1** (1 mmol), reductant [hydrazine monohydrate (0.5 mL)], and Pd–Au/TiO₂ nanoparticles (0.1 mol % of Pd–Au) were added. The resulting neat reaction mixture was stirred in an open vessel and at room temperature. The

progress of the reaction was monitored by thin-layer chromatography. After completion of the reaction, the reaction mixture was diluted with an aqueous NH₄Cl solution (approximately 10 mL) and extracted with ethyl acetate (3 × 3 mL). The organic layers were dried (Na₂SO₄) and concentrated under reduced pressure. Purification of the residue by silica gel column chromatography using petroleum ether/ethyl acetate as the eluent furnished the corresponding amines **2**, as a solid/viscous yellowish liquid.

Optimization of the Reaction Conditions. In order to find out the optimal reaction conditions, the hydrogenation of nitroarenes **1** (1 mmol) in the presence of various catalysts was studied in various parameters such as the effect of different conditions, and the results are summarized in Table 1. Initially, the reaction was carried out on nitrobenzene **1a** with hydrazine monohydrate as the reductant under solvent-free conditions, with different Zn-based mono/bimetallic catalysts such as ZnO, Zn_{0.7}Mn_{0.3}O_{2–δ}, and Zn_{0.7}Fe_{0.3}O_{2–δ} (Table 1, entries 1–3). However, no progress was noticed except for the recovery of the starting material. The reaction did not show any progress even with other metal transition-metal oxides NiFe₂O₄, CuFe₂O₄, SnO₂, and TiO₂ (Table 1, entries 4–7). On the other hand, the reaction with Pd/C furnished aniline **2a** in moderate yields (Table 1, entry 8). Notably, the reduction reaction in the presence of Pd/TiO₂ and Au/TiO₂ proved to be efficient and gave product **2a** in 82 and 80% yields, respectively, in shorter reaction times (Table 1, entries 9 & 10). Gratifyingly, the bimetallic Pd–Au/TiO₂ nanocatalyst turned out to be the best and afforded aniline **2a** just in 5 min in excellent yields under mild and solvent-free open vessel conditions (Table 1, entry 11). The catalytic activity of the catalyst depends on strong metal–support interaction (SMSI). The small size metal nanoparticles have more SMSI effect compared with large size metal nanoparticles.^{65,66} Therefore, Pd–Au/TiO₂ exhibited high catalytic activity due to small size of Pd–Au nanoparticles (for particles size see Figure S7).

The reaction was also explored with various solvents, such as methanol, ethanol, dichloromethane (DCM), ethyl acetate, and water, as depicted in Table 2. The protic solvents such as

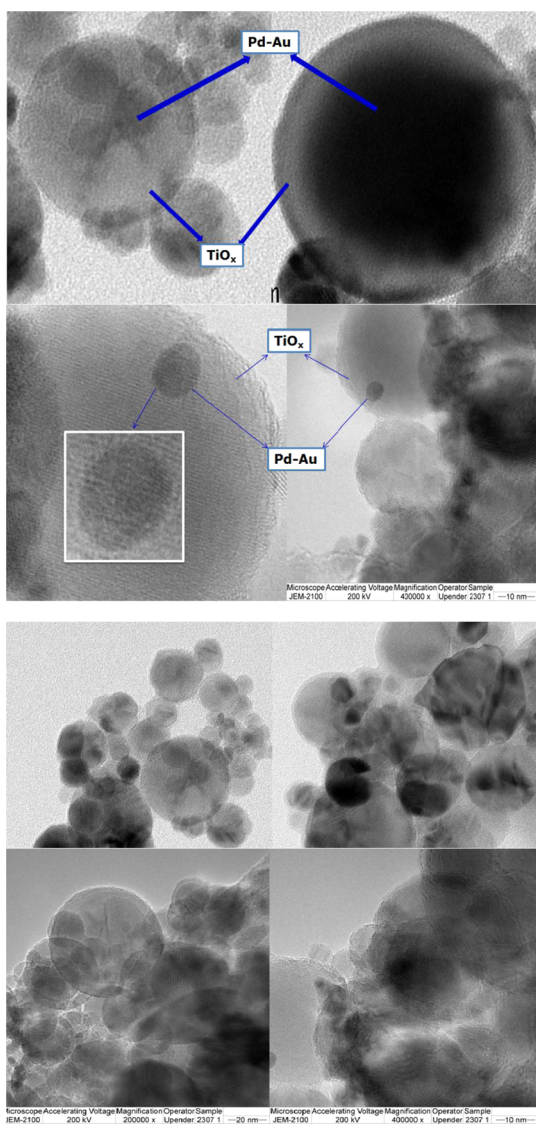


Figure 4. TEM images of as-prepared Pd–Au/TiO₂.

MeOH and EtOH seemed to be good and furnished **2a** in very good yields (Table 2, entries 1 & 2), whereas the solvents DCM and ethyl acetate were also good (Table 2, entries 3 & 4). Water was also found to be the useful solvent (Table 2, entry 5). On the other hand, the reaction with other reductants, such as NaBH₄ and H₂ balloon, furnished the product aniline **2a** in 76 and 64% yields, respectively (Table 2, entries 6 & 7).

Further to optimize the reaction with regard to the amount of hydrazine monohydrate (N₂H₄·H₂O), for the formation of aniline **2a**, it was planned to carry out the reduction on nitrobenzene **1a** with varying amounts of N₂H₄·H₂O. Thus, the reaction was carried out with 0.1, 0.2, 0.3, 0.4, and 0.5 mL of hydrazine monohydrate (N₂H₄·H₂O) for 10 min at room temperature and in an open vessel. However, it was observed that product yields were less with 0.1, 0.2, 0.3, and 0.4 mL of N₂H₄·H₂O when compared to that of 0.5 mL of N₂H₄·H₂O (Table 3, entries 1–5). Therefore, it was concluded that Pd–Au/TiO₂ (0.1 mol %) and N₂H₄·H₂O (0.5 mL) under the mild open vessel and solvent-free reaction conditions were best for the formation of aniline **2a** reduction (Table 1, entry 11).

Table 1. Catalyst Optimization Studies for the Formation of Aniline **2a**^a

entry	catalyst (mol %)	time	yield 2a (%) ^b
1	ZnO (2.5 mol %)	12 h	^c
2	Zn _{0.7} Mn _{0.3} O _{2-δ} (2.5 mol %)	12 h	^c
3	Zn _{0.7} Fe _{0.3} O _{2-δ} (2.5 mol %)	12 h	^c
4	NiFe ₂ O ₄ (2.5 mol %)	12 h	^c
5	CuFe ₂ O ₄ (2.5 mol %)	12 h	^c
6	SnO ₂ (2.5 mol %)	12 h	^c
7	TiO ₂ (2.5 mol %)	12 h	^c
8 ^d	Pd/C (2.5 mol %)	1 h	46
9	Pd/TiO ₂ (0.1 mol %)	15 min	82
10	Au/TiO ₂ (0.1 mol %)	10 min	80
11	Pd–Au/TiO ₂ (0.1 mol %)	5 min	96

^aReaction conditions: nitrobenzene (1 mmol), hydrazine monohydrate (0.5 mL), and catalyst. ^bIsolated yields of product **2a**. ^cStarting material **1a** recovered. ^dPd/C (palladium on activated charcoal).

Table 2. Solvent & Reductant Optimization Studies for the Formation of Aniline **2a**^a

entry	reductant	solvent	yield 2a (%) ^b
1	N ₂ H ₄ ·H ₂ O	MeOH	82
2	N ₂ H ₄ ·H ₂ O	EtOH	85
3	N ₂ H ₄ ·H ₂ O	DCM	75
4	N ₂ H ₄ ·H ₂ O	EA	76
5	N ₂ H ₄ ·H ₂ O	water	84
6	NaBH ₄	water	76
7 ^c	H ₂ balloon	water	64

^aReaction conditions: nitrobenzene (1 mmol), hydrazine monohydrate (0.5 mL), NaBH₄ (10 mmol), Pd–Au/TiO₂ (0.1 mol % of Pd–Au), and solvent (1 mL). ^bIsolated yields of product **2a**. ^cClosed vessel with atmospheric pressure.

Table 3. Optimization with Regard to the Amount of Reductant for the Formation of Aniline **2a**^a

entry	N ₂ H ₄ ·H ₂ O (mL)	yield 2a (%) ^b
1	0.1	65
2	0.2	72
3	0.3	80
4	0.4	85
5	0.5	96

^aReaction conditions: nitrobenzene (1 mmol) and Pd–Au/TiO₂ (0.1 mol % of Pd–Au). ^bIsolated yields of product **2a**.

With these best conditions in hand (Table 1, entry 11), next, to check the scope and generality of the method, the hydrogenation reaction was explored with various nitroarenes **1a–r**. Gratifyingly, the reaction was found to be amenable and

Table 4. Synthesis of Anilines 2a–i from Nitroarenes 1a–r^{a,b}

Entry	Substrate (1)	Product (2)	Time (min)	Yield 2 (%) ^b	Entry	Substrate (1)	Product (2)	Time (min)	Yield 2 (%) ^b
1			5	96	10			10	87
2			5	95	11			60	75
3			5	93	12			60	72
4			30	82	13			60	67
5			30	78	14			10	75
6			10	85	15			30	78
7			10	83	16			30	76
8			10	88	17			60	68
9			10	90	18			60	72

^aReaction conditions: nitrobenzene (1 mmol), hydrazine monohydrate (0.5 mL), and Pd–Au/TiO₂ (0.1 mol % of Pd–Au). ^bIsolated yields of product 2a–r.

afforded the corresponding amines 2a–i, in good to excellent yields (Table 4). Significantly, the reaction was completed in a reasonably short span of time. Interestingly, the reaction was successful with simple and methyl-substituted nitrobenzenes 1a–c and furnished the reduced anilines 2a–c in excellent yields (Table 4). However, the reaction with halo-substituted nitrobenzenes 1c–l (i.e. with Cl, Br, and I) not only reduced the nitro group but also removed the halide moieties reductively and thus furnished the products 2a–c in good to very good yields (Table 4). The reductive removal of halide groups along with the reduction of nitro functionality is due to the reactive nature of the catalyst. Quite interestingly, when the chloride/fluoride functionality belongs to other aromatic of biaryl nitro compound, the reduction was found to be chemoselective and gave the corresponding biaryl amines without affecting the halide moiety (Table 4, 2m–n). Though the exact reason is not certain at this stage on the selective reduction of the nitro group, however, this could be due to the reason that chloride is farther away from the nitro group and hence may be relatively less reactive. Notably, the reaction was compatible with benzylic bromo and hydroxyl groups (Table 4, 2o–p). In addition, the reaction was also found to be feasible

with nitroanilines 1q–r and yielded the products 2q–r in good yields (Table 4).

To further check the compatibility and applicability of the method, it was aimed to explore the reduction reaction with other nitroarenes. Thus, the reaction was performed on aldehyde-, ketone-, ester-, and double and triple bond-containing nitroarenes 1s–w (Table 5). To our delight, the method showed excellent compatibility and chemoselectivity and furnished the corresponding anilines 2s–w without affecting the aldehyde, ketone, ester, olefin, and alkyne groups (Table 5). Thus, this reveals the importance of the present protocol.

It is worth mentioning that the catalyst retains its activity, which is evident with nearly no loss of activity even after the fifth reaction cycle (Figure 5). This was done by recovering the catalyst by centrifugation and washing with ethyl acetate and acetone, followed by drying in a hot air oven at 60 °C for 12 h. The recovered Pd–Au/TiO₂ nanocatalyst was then subjected to the next catalytic cycles. The marginal loss of activity after the fifth cycle (<3%) may be due to loss of some amount of the catalyst during the recovery of the Pd–Au/TiO₂ nanocatalyst. The catalyst was recycled five times without an appreciable change in the product 2a yield, under the established

Table 5. Chemoselective Synthesis of Anilines 2s–w from Nitroarenes 1s–w^{a,b}

Entry	Substrate (1)	Product (2)	Time (min)	Yield 2 (%) ^b
19			15	89
20			15	82
21			5	72
22			5	68
23			5	70

^aReaction conditions: nitrobenzene (1 mmol), hydrazine monohydrate (0.5 mL), and Pd–Au/TiO₂ (0.1 mol % of Pd–Au). ^bIsolated yields of product 2s–w.

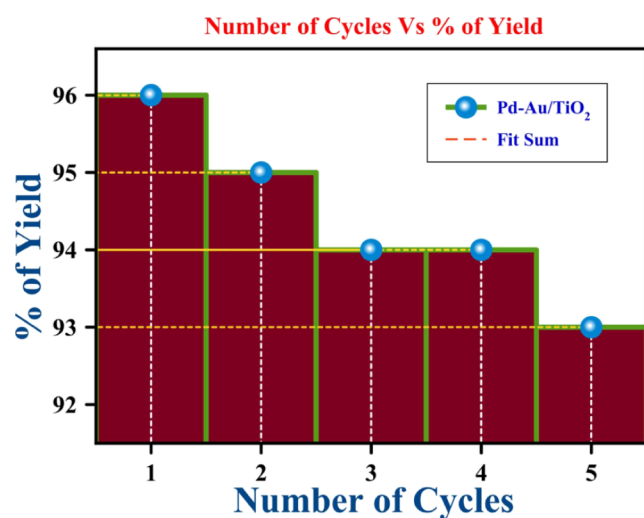
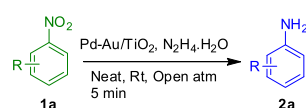


Figure 5. Recyclability of the Pd–Au/TiO₂ nanocatalyst in nitrobenzene hydrogenation reaction.

conditions. Thus, on the basis of the above results, it was confirmed that the Pd–Au/TiO₂ nanocatalyst is stable enough and can be reused.

CONCLUSION

In summary, we did a comparative study with as-synthesized various nanomaterials among all the catalysts and bimetallic Pd–Au nanoparticles impregnated on TiO₂ were found to exhibit excellent catalytic activity for various nitroarenes rapid hydrogenation reactions. On the other hand, this catalyst exhibits chemoselective nitroarenes hydrogenation under green atmospheric conditions. The Pd–Au/TiO₂ catalyst could be reused several times without any loss of activity. Typical results indicated the heterogeneous nature of the catalyst with good reusability.

EXPERIMENTAL SECTION

Instruments Used. Structural characterization of the catalyst was done on PANalytical, X'pertPRO with Cu K α radiation. Raman spectroscopy also corroborated the various phases of TiO₂ and thus the confirmation of various phases of TiO₂ was done by using Raman spectroscopy. Raman spectroscopy is analyzed in the Raman shift ranging from 70 to 900 cm^{−1} at the excitation line of 532 nm at room temperature. The oxidation state and the elemental composition of the as-prepared catalyst were confirmed by XPS with a

Kratos axis ultra-spectrometer with an Al K α source at 1498.5 eV, by fixing the emission current and applied a voltage at 10 mA and 15 kV. The weight percentages of metals in the catalysts were confirmed by X-ray fluorescence spectrometry and energy-dispersive X-ray spectroscopy. High-resolution TEM was performed by using a JEOL JEM 2100FX TEM instrument. ^1H & ^{13}C NMR spectra were recorded using a Bruker AVANCE instrument 400 & 100 MHz, respectively.

■ ASSOCIATED CONTENT

● Supporting Information

The Supporting Information is available free of charge on the ACS Publications website at DOI: 10.1021/acsomega.8b02064.

Details of catalyst synthesis and characterization studies and ^1H , ^{13}C NMR spectra of all isolated products (PDF)

■ AUTHOR INFORMATION

Corresponding Authors

*E-mail: gvsatya@iith.ac.in (G.S.).

*E-mail: csubbu@iith.ac.in (C.S.).

ORCID

Gedu Satyanarayana: 0000-0002-6410-5421

Challapalli Subrahmanyam: 0000-0002-2643-3854

Notes

The authors declare no competing financial interest.

■ ACKNOWLEDGMENTS

B.L. would like to thank the University Grant Commission (UGC), New Delhi, for awarding Junior & Senior Research Fellowship (JRF & SRF).

■ REFERENCES

- (1) Wang, D.; Astruc, D. Fast-growing field of magnetically recyclable nanocatalysts. *Chem. Rev.* **2014**, *114*, 6949–6985.
- (2) Jamatia, R.; Gupta, A.; Pal, A. K. Ru-Ferrite-Decorated Graphene (RuFG): A Sustainable and Efficient Catalyst for Conversion of Aromatic Aldehydes and Nitriles to Primary Amides in Aqueous Medium. *ACS Sustainable Chem. Eng.* **2017**, *5*, 7604–7612.
- (3) Narayana, B. L.; Mukri, B. D.; P, G.; Ch, S. Mn Ion substituted CeO₂Nano spheres for Low Temperature CO Oxidation: The Promoting Effect of Mn Ions. *ChemistrySelect* **2016**, *1*, 3150–3158.
- (4) Polshettiwar, V.; Luque, R.; Fihri, A.; Zhu, H.; Bouhrara, M.; Basset, J.-M. Magnetically recoverable nanocatalysts. *Chem. Rev.* **2011**, *111*, 3036–3075.
- (5) Lakshminarayana, B.; Mahendar, L.; Ghosal, P.; Satyanarayana, G.; Subrahmanyam, C. Nano-sized Recyclable PdO Supported Carbon Nanostructures for Heck Reaction: Influence of Carbon Materials. *ChemistrySelect* **2017**, *2*, 2700–2707.
- (6) Fountoulaki, S.; Daikopoulou, V.; Gkizis, P. L.; Tamiolakis, I.; Armatas, G. S.; Lykakis, I. N. Mechanistic Studies of the Reduction of Nitroarenes by NaBH₄ or Hydrosilanes Catalyzed by Supported Gold Nanoparticles. *ACS Catal.* **2014**, *4*, 3504–3511.
- (7) Tamiolakis, I.; Fountoulaki, S.; Vordos, N.; Lykakis, I. N.; Armatas, G. S. Mesoporous Au-TiO₂ nanoparticle assemblies as efficient catalysts for the chemoselective reduction of nitro compounds. *J. Mater. Chem. A* **2013**, *1*, 14311–14319.
- (8) Seth, J.; Kona, C. N.; Das, S.; Prasad, B. L. V. A simple method for the preparation of ultra-small palladium nanoparticles and their utilization for the hydrogenation of terminal alkyne groups to alkanes. *Nanoscale* **2015**, *7*, 872–876.
- (9) Seth, J.; Prasad, B. L. V. Bromide ion mediated modification to digestive ripening process: Preparation of ultra-small Pd, Pt, Rh and Ru nanoparticles. *Nano Res.* **2016**, *9*, 2007–2017.

- (10) Stamenkovic, V. R.; Mun, B. S.; Arenz, M.; Mayrhofer, K. J. J.; Lucas, C. A.; Wang, G.; Ross, P. N.; Markovic, N. M. Trends in electrocatalysis on extended and nanoscale Pt-bimetallic alloy surfaces. *Nat. Mater.* **2007**, *6*, 241–247.

- (11) Chen, G.; Desinan, S.; Rosei, R.; Rosei, F.; Ma, D. Synthesis of Ni-Ru Alloy Nanoparticles and Their High Catalytic Activity in Dehydrogenation of Ammonia Borane. *Chem.—Eur. J.* **2012**, *18*, 7925–7930.

- (12) Stratakis, M.; Garcia, H. Catalysis by supported gold nanoparticles: beyond aerobic oxidative processes. *Chem. Rev.* **2012**, *112*, 4469–4506.

- (13) Corma, A.; Leyva-Pérez, A.; Sabater, M. J. Gold-Catalyzed Carbon–Heteroatom Bond-Forming Reactions. *Chem. Rev.* **2011**, *111*, 1657–1712.

- (14) Lu, Y.; Yuan, J.; Polzer, F.; Drechsler, M.; Preussner, J. In Situ Growth of Catalytic Active Au–Pt Bimetallic Nanorods in Thermoresponsive Core–Shell Microgels. *ACS Nano* **2010**, *4*, 7078–7086.

- (15) Budroni, G.; Corma, A. Gold and gold-platinum as active and selective catalyst for biomass conversion: Synthesis of γ -butyrolactone and one-pot synthesis of pyrrolidone. *J. Catal.* **2008**, *257*, 403–408.

- (16) Byun, S.; Song, Y.; Kim, B. M. Heterogenized Bimetallic Pd–Pt–Fe₃O₄ Nanoflakes as Extremely Robust, Magnetically Recyclable Catalysts for Chemoselective Nitroarene Reduction. *ACS Appl. Mater. Interfaces* **2016**, *8*, 14637–14647.

- (17) Zhang, J.; Chen, G.; Guay, D.; Chaker, M.; Ma, D. Highly active PtAu alloy nanoparticle catalysts for the reduction of 4-nitrophenol. *Nanoscale* **2014**, *6*, 2125–2130.

- (18) Zhang, Y.; Zhang, N.; Tang, Z.-R.; Xu, Y.-J. Graphene Oxide as a Surfactant and Support for In-Situ Synthesis of Au–Pd Nanoalloys with Improved Visible Light Photocatalytic Activity. *J. Phys. Chem. C* **2014**, *118*, 5299–5308.

- (19) Yang, M.-Q.; Pan, X.; Zhang, N.; Xu, Y.-J. A facile one-step way to anchor noble metal (Au, Ag, Pd) nanoparticles on a reduced graphene oxide mat with catalytic activity for selective reduction of nitroaromatic compounds. *CrystEngComm* **2013**, *15*, 6819–6828.

- (20) Cui, X.; Long, Y.; Zhou, X.; Yu, G.; Yang, J.; Yuan, M.; Ma, J.; Dong, Z. Pd-doped Ni nanoparticle-modified N-doped carbon nanocatalyst with high Pd atom utilization for the transfer hydrogenation of nitroarenes. *Green Chem.* **2018**, *20*, 1121–1130.

- (21) Yang, J.; Wang, W. D.; Dong, Z. PdCo nanoparticles supported on carbon fibers derived from cotton: Maximum utilization of Pd atoms for efficient reduction of nitroarenes. *J. Colloid Interface Sci.* **2018**, *524*, 84–92.

- (22) Tian, M.; Cui, X.; Yuan, M.; Yang, J.; Ma, J.; Dong, Z. Efficient chemoselective hydrogenation of halogenated nitrobenzenes over an easily prepared γ -Fe₂O₃-modified mesoporous carbon catalyst. *Green Chem.* **2017**, *19*, 1548–1554.

- (23) Yang, M.-Q.; Weng, B.; Xu, Y.-J. Synthesis of In₂S₃-CNT nanocomposites for selective reduction under visible light. *J. Mater. Chem. A* **2014**, *2*, 1710–1720.

- (24) Sorribes, I.; Liu, L.; Corma, A. Nanolayered Co–Mo–S Catalysts for the Chemoselective Hydrogenation of Nitroarenes. *ACS Catal.* **2017**, *7*, 2698–2708.

- (25) Zhou, J.; Li, Y.; Sun, H.-b.; Tang, Z.; Qi, L.; Liu, L.; Ai, Y.; Li, S.; Shao, Z.; Liang, Q. Porous silica-encapsulated and magnetically recoverable Rh NPs: a highly efficient, stable and green catalyst for catalytic transfer hydrogenation with “slow-release” of stoichiometric hydrazine in water. *Green Chem.* **2017**, *19*, 3400–3407.

- (26) Wu, Z.; Jiang, H. Efficient palladium and ruthenium nanocatalysts stabilized by phosphine functionalized ionic liquid for selective hydrogenation. *RSC Adv.* **2015**, *5*, 34622–34629.

- (27) Wei, Z.; Thushara, D.; Li, X.; Zhang, Z.; Liu, Y.; Lu, X. Ligand-controlled fabrication of core-shell PdNi bimetallic nanoparticles as a highly efficient hydrogenation catalyst. *Catal. Commun.* **2017**, *98*, 61–65.

- (28) Yu, L.; Zhang, Q.; Li, S.-S.; Huang, J.; Liu, Y.-M.; He, H.-Y.; Cao, Y. Gold-Catalyzed Reductive Transformation of Nitro

Compounds Using Formic Acid: Mild, Efficient, and Versatile. *ChemSusChem* **2015**, *8*, 3029–3035.

(29) Krogul, A.; Litwinienko, G. Application of Pd(II) Complexes with Pyridines as Catalysts for the Reduction of Aromatic Nitro Compounds by CO/H₂O. *Org. Process Res. Dev.* **2015**, *19*, 2017–2021.

(30) Yang, S.-T.; Shen, P.; Liao, B.-S.; Liu, Y.-H.; Peng, S.-M.; Liu, S.-T. Catalytic Reduction of Nitroarenes by Dipalladium Complexes: Synergistic Effect. *Organometallics* **2017**, *36*, 3110–3116.

(31) Schabel, T.; Belger, C.; Plietker, B. A mild chemoselective Ru-catalyzed reduction of alkynes, ketones, and nitro compounds. *Org. Lett.* **2013**, *15*, 2858–2861.

(32) Maeno, Z.; Mitsudome, T.; Mizugaki, T.; Jitsukawa, K.; Kaneda, K. Selective synthesis of Rh₅ carbonyl clusters within a polyamine dendrimer for chemoselective reduction of nitro aromatics. *Chem. Commun.* **2014**, *50*, 6526–6529.

(33) Chen, S.; Lu, G.; Cai, C. Iridium-catalyzed transfer hydrogenation of nitroarenes to anilines. *New J. Chem.* **2015**, *39*, 5360–5365.

(34) Vijaykumar, G.; Mandal, S. K. An abnormal N-heterocyclic carbene based nickel complex for catalytic reduction of nitroarenes. *Dalton Trans.* **2016**, *45*, 7421–7426.

(35) Mandal, P. K.; McMurray, J. S. Pd–C-Induced Catalytic Transfer Hydrogenation with Triethylsilane. *J. Org. Chem.* **2007**, *72*, 6599–6601.

(36) Govan, J.; Gun'ko, Y. Recent advances in the application of magnetic nanoparticles as a support for homogeneous catalysts. *Nanomaterials* **2014**, *4*, 222–241.

(37) Zhang, N.; Xu, Y.-J. Aggregation- and Leaching-Resistant, Reusable, and Multifunctional Pd@CeO₂ as a Robust Nanocatalyst Achieved by a Hollow Core-Shell Strategy. *Chem. Mater.* **2013**, *25*, 1979–1988.

(38) Chen, J.; Yao, M.; Wang, X. Investigation of transition metal ion doping behaviors on TiO₂ nanoparticles. *J. Nanopart. Res.* **2008**, *10*, 163–171.

(39) Swapna, M. V.; Haridas, K. R. Sonochemical Synthesis and Morphological Study of Nanocrystalline Rutile TiO₂. *J. Am. Inst. Chem.* **2015**, *88*, 1–6.

(40) Zheng, K.; Zhang, T.-c.; Lin, P.; Han, Y.-h.; Li, H.-y.; Ji, R.-j.; Zhang, H.-y. 4-Nitroaniline Degradation by TiO₂Catalyst Doping with Manganese. *J. Chem.* **2015**, *2015*, 1–6.

(41) Liu, J.; Guo, Q.; Yu, M.; Li, S. Effect of TiO₂ nanostructures on specific capacitance of Al₂O₃-TiO₂ composite film on etched aluminum foil formed by the sol-gel and anodizing. *Ceram. Int.* **2014**, *40*, 3687–3692.

(42) Haque, F. Z.; Nandanwar, R.; Singh, P. Evaluating photo-degradation properties of anatase and rutile TiO₂ nanoparticles for organic compounds. *Optik* **2017**, *128*, 191–200.

(43) Geraldine, A. N.; Silva, D. F.; Silva, J. C. M.; Souza, R. F. B.; Spinacé, E. V.; Neto, A. O.; Linardi, M.; Santos, M. C. Glycerol electrooxidation in alkaline medium using Pd/C, Au/C and PdAu/C electrocatalysts prepared by electron beam irradiation. *J. Braz. Chem. Soc.* **2014**, *25*, 831–840.

(44) Lubas, M.; Jasinski, J. J.; Sitarz, M.; Kurpaska, L.; Podsiad, P.; Jasinski, J. Raman spectroscopy of TiO₂ thin films formed by hybrid treatment for biomedical applications. *Spectrochim. Acta, Part A* **2014**, *133*, 867–871.

(45) Mazza, T.; Barborini, E.; Piseri, P.; Milani, P.; Cattaneo, D.; Bassi, A. L.; Ducati, C. Raman spectroscopy characterization of TiO₂ rutile nanocrystals. *Phys. Rev. B: Condens. Matter Mater. Phys.* **2007**, *75*, 045416.

(46) Nunes, D.; Pimentel, A.; Santos, L.; Barquinha, P.; Fortunato, E.; Martins, R. Photocatalytic TiO₂ Nanorod Spheres and Arrays Compatible with Flexible Applications. *Catalysts* **2017**, *7*, 60.

(47) Wang, Y.; Li, L.; Huang, X.; Li, Q.; Li, G. New insights into fluorinated TiO₂ (brookite, anatase and rutile) nanoparticles as efficient photocatalytic redox catalysts. *RSC Adv.* **2015**, *5*, 34302–34313.

(48) Meinhold, G. Rutile and its applications in earth sciences. *Earth-Sci. Rev.* **2010**, *102*, 1–28.

(49) Choudhury, B.; Verma, R.; Choudhury, A. Oxygen defect assisted paramagnetic to ferromagnetic conversion in Fe doped TiO₂nanoparticles. *RSC Adv.* **2014**, *4*, 29314–29323.

(50) Verma, R.; Gangwar, J.; Srivastava, A. K. Multiphase TiO₂ nanostructures: a review of efficient synthesis, growth mechanism, probing capabilities, and applications in bio-safety and health. *RSC Adv.* **2017**, *7*, 44199–44224.

(51) Reis, É. M.; de Rezende, A. A. A.; de Oliveira, P. F.; Nicoletta, H. D.; Tavares, D. C.; Silva, A. C. A.; Dantas, N. O.; Spanó, M. A. Evaluation of titanium dioxide nanocrystal-induced genotoxicity by the cytokinesis-block micronucleus assay and the *Drosophila* wing spot test. *Food Chem. Toxicol.* **2016**, *96*, 309–319.

(52) Xu, J.; Wu, S.; Ri, J. H.; Jin, J.; Peng, T. Bilayer film electrode of brookite TiO₂ particles with different morphology to improve the performance of pure brookite-based dye-sensitized solar cells. *J. Power Sources* **2016**, *327*, 77–85.

(53) El-Sheikh, S. M.; Khedr, T. M.; Hakki, A.; Ismail, A. A.; Badawy, W. A.; Bahnemann, D. W. Visible light activated carbon and nitrogen co-doped mesoporous TiO₂ as efficient photocatalyst for degradation of ibuprofen. *Sep. Purif. Technol.* **2017**, *173*, 258–268.

(54) El-Sheikh, S. M.; Khedr, T. M.; Zhang, G.; Vogiaz, V.; Ismail, A. A.; O'Shea, K.; Dionysiou, D. D. Tailored synthesis of anatase-brookite heterojunction photocatalysts for degradation of cyndrospermopsin under UV-Vis light. *Chem. Eng. J.* **2017**, *310*, 428–436.

(55) Mahoney, L.; Koodali, R. Versatility of Evaporation-Induced Self-Assembly (EISA) Method for Preparation of Mesoporous TiO₂ for Energy and Environmental Applications. *Materials* **2014**, *7*, 2697–2746.

(56) Shaikh, S. F.; Mane, R. S.; Min, B. K.; Hwang, Y. J.; Joo, O.-S. D-sorbitol-induced phase control of TiO₂ nanoparticles and its application for dye-sensitized solar cells. *Sci. Rep.* **2016**, *6*, 20103.

(57) Swamy, V. Size-dependent modifications of the first-order Raman spectra of nanostructured rutile TiO₂. *Phys. Rev. B: Condens. Matter Mater. Phys.* **2008**, *77*, 195414.

(58) Kumar, S. G.; Rao, K. S. R. K. Polymorphic phase transition among the titania crystal structures using a solution-based approach: from precursor chemistry to nucleation process. *Nanoscale* **2014**, *6*, 11574–11632.

(59) Buonsanti, R.; Grillo, V.; Carlino, E.; Giannini, C.; Kipp, T.; Cingolani, R.; Cozzoli, P. D. Nonhydrolytic Synthesis of High-Quality Anisotropically Shaped Brookite TiO₂Nanocrystals. *J. Am. Chem. Soc.* **2008**, *130*, 11223–11233.

(60) Lakshminarayana, B.; Mahendar, L.; Ghosal, P.; Sreedhar, B.; Satyanarayana, G.; Subrahmanyam, C. Fabrication of Pd/CuFe₂O₄ hybrid nanowires: a heterogeneous catalyst for Heck couplings. *New J. Chem.* **2018**, *42*, 1646–1654.

(61) Ke, X.; Zhang, X.; Zhao, J.; Sarina, S.; Barry, J.; Zhu, H. Selective reductions using visible light photocatalysts of supported gold nanoparticles. *Green Chem.* **2013**, *15*, 236–244.

(62) Al-Omani, S. J.; Bumajdad, A.; Al Sagheer, F. A.; Zaki, M. I. Surface and related bulk properties of titania nanoparticles recovered from aramid-titania hybrid films: A novel attempt. *Mater. Res. Bull.* **2012**, *47*, 3308–3316.

(63) De Bonis, A.; Galasso, A.; Ibris, N.; Laurita, A.; Santagata, A.; Teghil, R. Rutile microtubes assembly from nanostructures obtained by ultra-short laser ablation of titanium in liquid. *Appl. Surf. Sci.* **2013**, *268*, 571–578.

(64) Huang, C.-N.; Bow, J.-S.; Zheng, Y.; Chen, S.-Y.; Ho, N. J.; Shen, P. Nonstoichiometric titanium oxides via pulsed laser ablation in water. *Nanoscale Res. Lett.* **2010**, *5*, 972–985.

(65) Coq, B.; Dutartre, R.; Figueras, F.; Tazi, T. Particle size, precursor, and support effects in the hydrogenolysis of alkanes over supported rhodium catalysts. *J. Catal.* **1990**, *122*, 438–447.

(66) Jiang, F.; Cai, J.; Liu, B.; Xu, Y.; Liu, X. Particle size effects in the selective hydrogenation of cinnamaldehyde over supported palladium catalysts. *RSC Adv.* **2016**, *6*, 75541–75551.